RA–RAR-β counteracts myelin-dependent inhibition of neurite outgrowth via Lingo-1 repression

Radhika Puttagunta,[1] André Schmandke,[1] Elisa Floriddia,[1,2] Perrine Gaub,[1,2] Natalie Fomin,[2] Norbert B. Ghyselinck,[3] and Simone Di Giovanni[1]

[1]Laboratory for NeuroRegeneration and Repair, Center for Neurology, Hertie Institute for Clinical Brain Research and [2]Graduate School for Cellular and Molecular Neuroscience, University of Tuebingen, 72074 Tuebingen, Germany
[3]Institut de Génétique et de Biologie Moléculaire et Cellulaire, Institut National de la Santé et de la Recherche Médicale U964, University Louis Pasteur de Strasbourg, 67081 Strasbourg, France

After an acute central nervous system injury, axonal regeneration is limited as the result of a lack of neuronal intrinsic competence and the presence of extrinsic inhibitory signals. The injury fragments the myelin neuronal insulating layer, releasing extrinsic inhibitory molecules to signal through the neuronal membrane–bound Nogo receptor (NgR) complex. In this paper, we show that a neuronal transcriptional pathway can interfere with extrinsic inhibitory myelin-dependent signaling, thereby promoting neurite outgrowth. Specifically, retinoic acid (RA), acting through the RA receptor β (RAR-β), inhibited myelin-activated NgR signaling through the transcriptional repression of the NgR complex member Lingo-1. We show that suppression of Lingo-1 was required for RA–RAR-β to counteract extrinsic inhibition of neurite outgrowth. Furthermore, we confirm in vivo that RA treatment after a dorsal column overhemisection injury inhibited Lingo-1 expression, specifically through RAR-β. Our findings identify a novel link between RA–RAR-β–dependent proaxonal outgrowth and inhibitory NgR complex–dependent signaling, potentially allowing for the development of molecular strategies to enhance axonal regeneration after a central nervous system injury.

Introduction

The neuronal insulating layer, myelin, is fragmented after a spinal lesion, releasing the extrinsic inhibitory molecules myelin-associated glycoprotein (MAG), Nogo, and oligodendrocyte myelin glycoprotein (He and Koprivica, 2004) that inhibit axonal outgrowth and functional recovery after injury. These myelin proteins signal through the neuronal membrane–bound Nogo receptor (NgR) complex, which includes NgR1 (Chen et al., 2000; GrandPré et al., 2000), Lingo-1 (Mi et al., 2004), and $p75^{NTR}$ (Domeniconi et al., 2002; Wong et al., 2002) or TROY (Park et al., 2005). Myelin protein engagement of the NgR complex activates RhoA, which induces Rho kinase–dependent phosphorylation of cofilin and, thus, actin depolymerization and growth cone collapse (He and Koprivica, 2004).

The NgR complex (Bregman et al., 1995; Thallmair et al., 1998; GrandPré et al., 2000; Merkler et al., 2001; Li and Strittmatter, 2003; Mi et al., 2004) is vital for growth cone collapse and inhibition of neurite outgrowth. Although both the up- and downstream components of NgR complex–dependent signaling have been extensively studied (He and Koprivica, 2004), the transcriptional regulation of its individual members remains unknown.

The overexpression of the transcription factor retinoic acid (RA) receptor β2 (RAR-β2) promotes neurite outgrowth in primary neurons cultured on inhibitory substrates and induces axonal regeneration via neuronal intrinsic pathways in vivo after a spinal lesion (Wong et al., 2006; Yip et al., 2006). More recently, phosphorylated AKT, a serine/threonine kinase, was associated with the beneficial effects of RAR-β2 (Agudo et al., 2010); however, thus far, no direct transcriptional targets for RAR-β2 that promote neurite outgrowth on inhibitory substrates have been identified.

Correspondence to Simone Di Giovanni: simone.digiovanni@medizin.uni-tuebingen.de

Abbreviations used in this paper: ANOVA, analysis of variance; CGN, cerebellar granular neuron; ChIP, chromatin IP; CSPG, chondroitin sulfate proteoglycan; IP, intraperitoneal; MAG, myelin-associated glycoprotein; NgR, Nogo receptor; PDL, poly-D-lysine; RA, retinoic acid; RAR-β, RA receptor β; RARE, RA response element; RXR, retinoid X receptor; SCI, spinal cord injury.

The Rockefeller University Press $30.00
J. Cell Biol. Vol. 193 No. 7 1147–1156
www.jcb.org/cgi/doi/10.1083/jcb.201102066

Importantly, transcriptional proneurite outgrowth and extrinsic inhibitory pathways have not been previously shown to directly intersect or form a unique signaling cascade. Here, we show that RA-bound RAR-β occupies a specific RA response element (RARE) on the Lingo-1 promoter, transcriptionally repressing Lingo-1 myelin-dependent gene activation. Furthermore, Lingo-1 expression is required for RA–RAR-β to counteract myelin-dependent inhibition of neurite outgrowth. Finally, we show in vivo that RA treatment after a dorsal column overhemisection lesion inhibits Lingo-1 expression, specifically through RAR-β. Our findings identify a novel pathway that specifically links the RA–RAR-β–dependent proaxonal outgrowth and the inhibitory NgR complex–dependent signaling.

Results and discussion

RA–RAR-β counteracts myelin-dependent inhibition

We wanted to examine the RAR-β–dependent molecular pathways involved in neurite outgrowth in nonpermissive conditions after the administration of the clinically available all-trans RA, a lipophilic vitamin A derivative that readily transverses the blood–brain barrier (Le Doze et al., 2000). Cultured mouse cerebellar granular neurons (CGNs) were used as an in vitro neurite outgrowth model of the central nervous system (Dubreuil et al., 2003; Yamashita and Tohyama, 2003; Madura et al., 2004). When CGNs were cultured on poly-D-lysine (PDL) or PDL plus myelin substrate (henceforth myelin) with 1 µM RA (a dosage known to reach therapeutic levels in humans; Miano and Berk, 2000) or vehicle (DMSO) administered at the time of plating, we observed that RA promoted neurite outgrowth (approximately twofold) in CGNs on a nonpermissive myelin but not on a permissive PDL substrate (Fig. 1, A and B). Given that these effects may be influenced by cell survival, we examined cell survival between samples by the analysis of apoptotic nuclei and found no differences (Fig. S1 A). RAR-β is expressed in CGNs (Fig. S1 B) and may be the RAR relevant for RA-induced neurite outgrowth (Corcoran et al., 2002). Therefore, neurite outgrowth experiments were performed in RAR-$\beta^{-/-}$ CGNs to investigate whether RAR-β is essential to the ability of RA to counteract myelin-dependent inhibition of neurite outgrowth. Contrary to what we observed in wild-type CGNs, neurite outgrowth was no longer enhanced on myelin with RA in RAR-$\beta^{-/-}$ CGNs (Fig. 1, A and B).

The activation of RhoA is a classical downstream event in myelin-dependent activation of NgR signaling. When we plated wild-type CGNs on PDL with or without RA treatment for 24 h, at which time we added 1 µg/ml MAG for 15 min, we found that the RA-dependent increase in neurite outgrowth is associated with a decrease in RhoA activation (Fig. 1 C). It is also important to note that RA did not modify neurite outgrowth through RAR-β when CGNs were plated on another inhibitory substrate, chondroitin sulfate proteoglycans (CSPGs; Fig. S1 C), suggesting that RA–RAR-β functions by preferentially modulating myelin-dependent signaling.

RA–RAR-β represses the myelin-dependent induction of Lingo-1

To investigate whether RA–RAR-β is able to affect myelin-derived inhibitory signals by directly modulating the gene expression of the NgR complex members, we conducted an in silico analysis. We used a specific algorithm developed for transcription elements (Transcription Element Search System [TESS]) to identify RAREs on the promoters of NgR, Lingo-1, $p75^{NTR}$, and TROY. This led to the discovery of novel RAREs on both the Lingo-1 (a full site) and NgR (only half sites) promoters (Fig. 2 A), suggesting that they may be possible RA–RAR-β target genes. Therefore, we examined the gene expression of Lingo-1 and NgR, as well as the other NgR complex members, by real-time RT-PCR in wild-type and RAR-$\beta^{-/-}$ CGNs cultured on PDL or myelin, and we discovered that both Lingo-1 and NgR1 expression was increased in CGNs plated on myelin (Fig. 2 B). If RA transcriptionally regulated Lingo-1 and NgR expression on myelin via RAR-β, the delivery of RA would affect their gene expression in wild-type but not in RAR-$\beta^{-/-}$ CGNs. Indeed, myelin-induced Lingo-1 expression was repressed by RA in wild-type but not RAR-$\beta^{-/-}$ CGNs at 8 h and even further so at 24 h after plating (Fig. 2 C). Myelin also induced a significant increase in Lingo-1 protein expression, which was abrogated by RA treatment in wild-type but not RAR-$\beta^{-/-}$ CGNs (Fig. 2 D). The expression of NgR1 was not preferentially regulated through RA–RAR-β, as its gene expression was significantly affected by RA both in wild-type and RAR-$\beta^{-/-}$ CGNs (unpublished data). It is important to note that without Lingo-1, the NgR complex of NgR, Lingo-1, and $p75^{NTR}$ or TROY is unable to transmit myelin inhibitory signals (Mi et al., 2004; Park et al., 2005; Shao et al., 2005; Ji et al., 2006); therefore, modest yet significant changes in its expression can have profound effects. Also noteworthy, myelin transcriptional regulation of Lingo-1 appears to be independent of RA–RAR-β transcriptional regulation of Lingo-1 as observed by the increase in Lingo-1 expression in RAR-$\beta^{-/-}$, which is similar to that seen in wild-type CGNs. This indicates that the RA–RAR-β pathway is not responsible for Lingo-1 up-regulation by myelin. Altogether, these data suggest that Lingo-1 gene expression is induced by myelin and that RA–RAR-β acts as a repressor of the myelin-dependent gene induction of Lingo-1 through the possible binding to novel RAREs in its promoter.

RAR-β occupies a RARE on Lingo-1, repressing its expression

Typically, the nuclear receptor RAR-β bound by its ligand RA forms a heterodimer with the retinoid X receptor (RXR), binds to RAREs in gene promoters, and activates transcription (Chambon, 1996). However, there have been several documented cases in which RAR-β was found to occupy promoters independently from RXR and to repress transcription (Glass et al., 1989; Lipkin et al., 1992; Schoorlemmer et al., 1994).

To specifically explore whether RAR-β acts as a repressor of Lingo-1 gene expression, we electroporated both wild-type and RAR-$\beta^{-/-}$ CGNs cultured on PDL or myelin with human RAR-β2 in combination with RA or vehicle and measured Lingo-1 expression by real-time RT-PCR. In wild type,

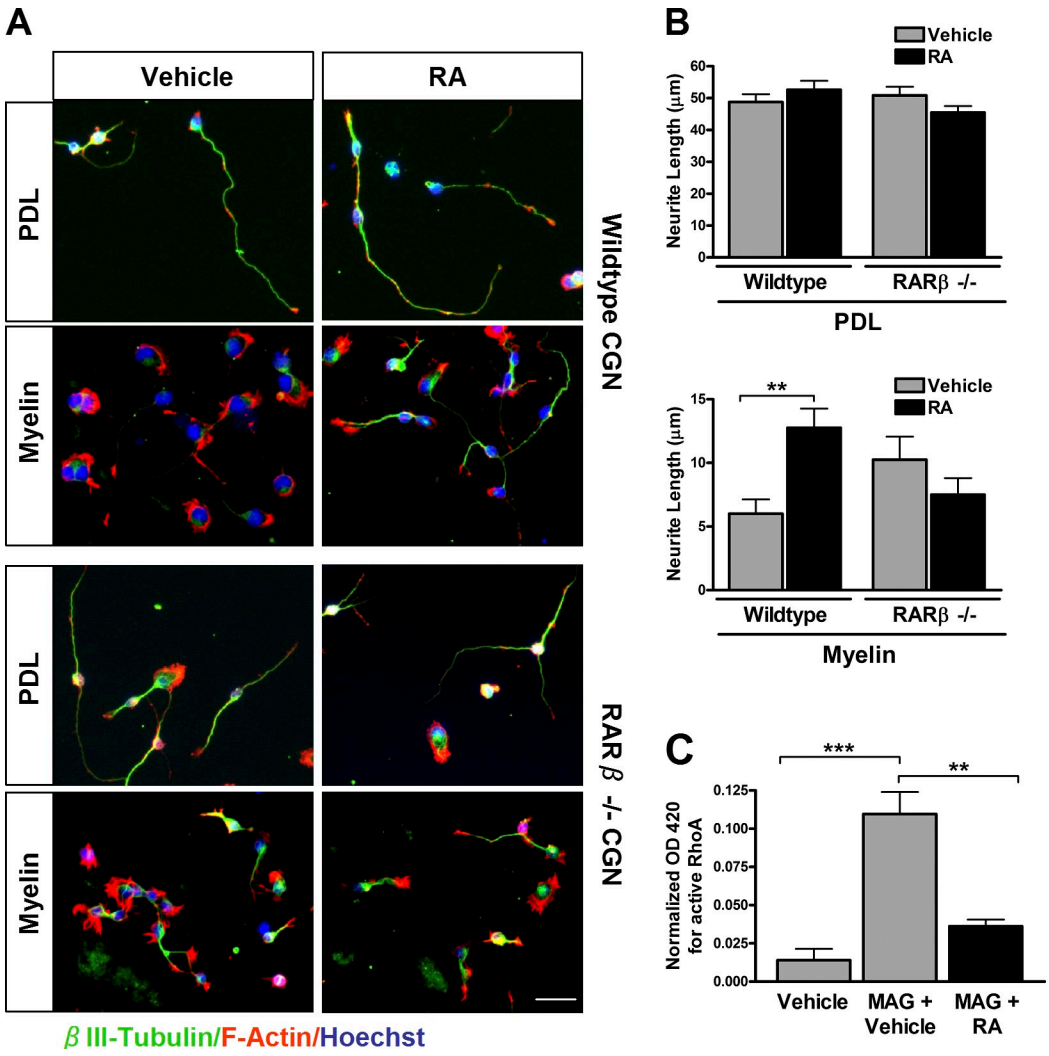

Figure 1. **RA–RAR-β counteracts myelin-dependent inhibition of neurite outgrowth through RhoA inhibition.** (A) Wild-type and RAR-$\beta^{-/-}$ CGNs cultured on PDL or myelin with vehicle or 1 μM RA for 24 h. Bar, 50 μm. (B) Quantification of neurite length. Myelin inhibition of neurite outgrowth was significantly counteracted in wild type, but not RAR-$\beta^{-/-}$, by RA. (C) Wild-type CGNs were stressed with MAG for 15 min. Strong induction of RhoA activation with MAG was significantly inhibited by prior 24-h RA treatment (n = 3). **, P < 0.01; ***, P < 0.001. Data are plotted as the mean ± SEM.

whereas RA treatment alone repressed Lingo-1 expression, RAR-β2 overexpression alone only partially repressed Lingo-1, but in combination with RA, it fully attenuated myelin-induced Lingo-1 expression (Fig. 3 A). In RAR-$\beta^{-/-}$, RA alone could not inhibit Lingo-1, likely as a result of the absence of basal RAR-β expression; however, exogenous overexpression of RAR-β2 alone inhibited myelin-induced Lingo-1 expression, an effect that was enhanced with additional RA treatment (Fig. 3 B). Subsequent chromatin immunoprecipitation (ChIP) experiments demonstrated that RAR-β specifically occupies the Lingo-1 in silico–predicted RARE1, but not the RARE2 (Fig. 3 C), in a chromatin environment (Fig. 3 D). Interestingly, Lingo-1 promoter occupancy was strongly enhanced by RA when CGNs were plated on myelin, whereas myelin itself reduced RAR-β occupancy in comparison with neurons on PDL (Fig. 3 D). As RAR-β occupies RAREs as a homodimer or as a heterodimer with RXR (Chambon, 1996; Vernet et al., 2006), we sought to determine whether RXR also underwent myelin- or RA-dependent changes in Lingo-1 promoter occupancy on the RARE1 or RARE2. To this end, we performed a ChIP with the RXR antibody that showed no change in myelin- or RA-dependent Lingo-1 promoter occupancy (Fig. 3 E), suggesting that myelin and RA specifically regulate RAR-β occupancy of the Lingo-1 promoter.

To determine whether RAR-β is a repressor of Lingo-1 transcription, luciferase assays were performed. The proximal Lingo-1 genomic region of ∼1,000 bp containing both the RARE1 and RARE2 was cloned into a luciferase vector driven by a cytomegalovirus promoter (Fig. 3 F). Because of the limited transfection efficiency of the luciferase vector in primary neurons, which strongly restricted the quality of the luciferase signal, luciferase assays were performed in neuroblastoma cells (previously shown to be responsive to RA and sensitive to myelin-dependent inhibition of neurite outgrowth; Caroni et al., 1988; Schwab and Caroni, 1988; Encinas et al., 1999; Merrill et al., 2004) transfected with RAR-β2 and plated on PDL or myelin. These experiments clearly demonstrate that Lingo-1 luciferase activity is enhanced by myelin as compared with PDL

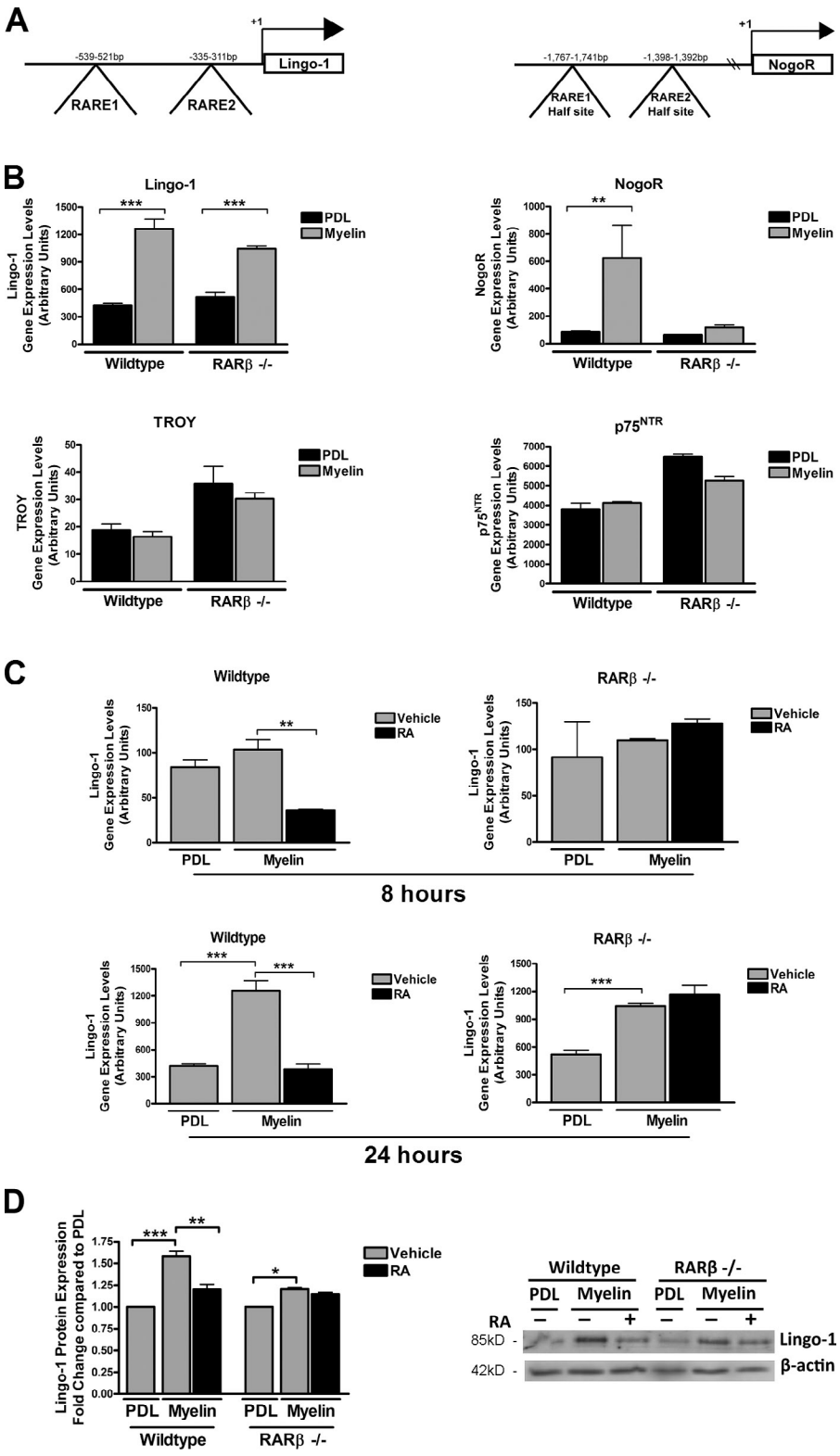

Figure 2. **RA–RAR-β represses the myelin-dependent induction of Lingo-1.** (A) A diagram of newly discovered RAREs in the Lingo-1 and NgR promoters. (B) Gene expression analysis of the NgR complex members from wild-type and RAR-$\beta^{-/-}$ CGNs on PDL and myelin. (C) Lingo-1 myelin-dependent gene expression is repressed by RA treatment in wild type but not RAR-$\beta^{-/-}$ for 8 and 24 h. (D) Protein expression analysis and representative immunoblot of Lingo-1 from CGNs. Myelin induced a significant increase in Lingo-1 protein expression, which was attenuated by 24-h RA treatment in wild type but not RAR-$\beta^{-/-}$ (n = 3). One-way ANOVA Bonferroni posttests: *, $P < 0.05$; **, $P < 0.01$; ***, $P < 0.001$. Data are plotted as the mean ± SEM.

and repressed by the administration of the ligand RA (Fig. 3 G). Furthermore, when the RARE1 that was shown to specifically bind RAR-β via a ChIP assay was mutated, there was no RA-dependent repression observed in luciferase activity on myelin (Fig. 3 G). These data also suggest that myelin-dependent induction of Lingo-1 expression must take effect within this 1,000-bp fragment but not within the RARE1, as myelin induced luciferase expression of both the Lingo-1 promoter and the mutant Lingo-1 promoter.

Together, we show for the first time that myelin strongly inhibits the recruitment of RAR-β to the RARE1 in the Lingo-1 promoter and that RA treatment allows RAR-β to occupy the

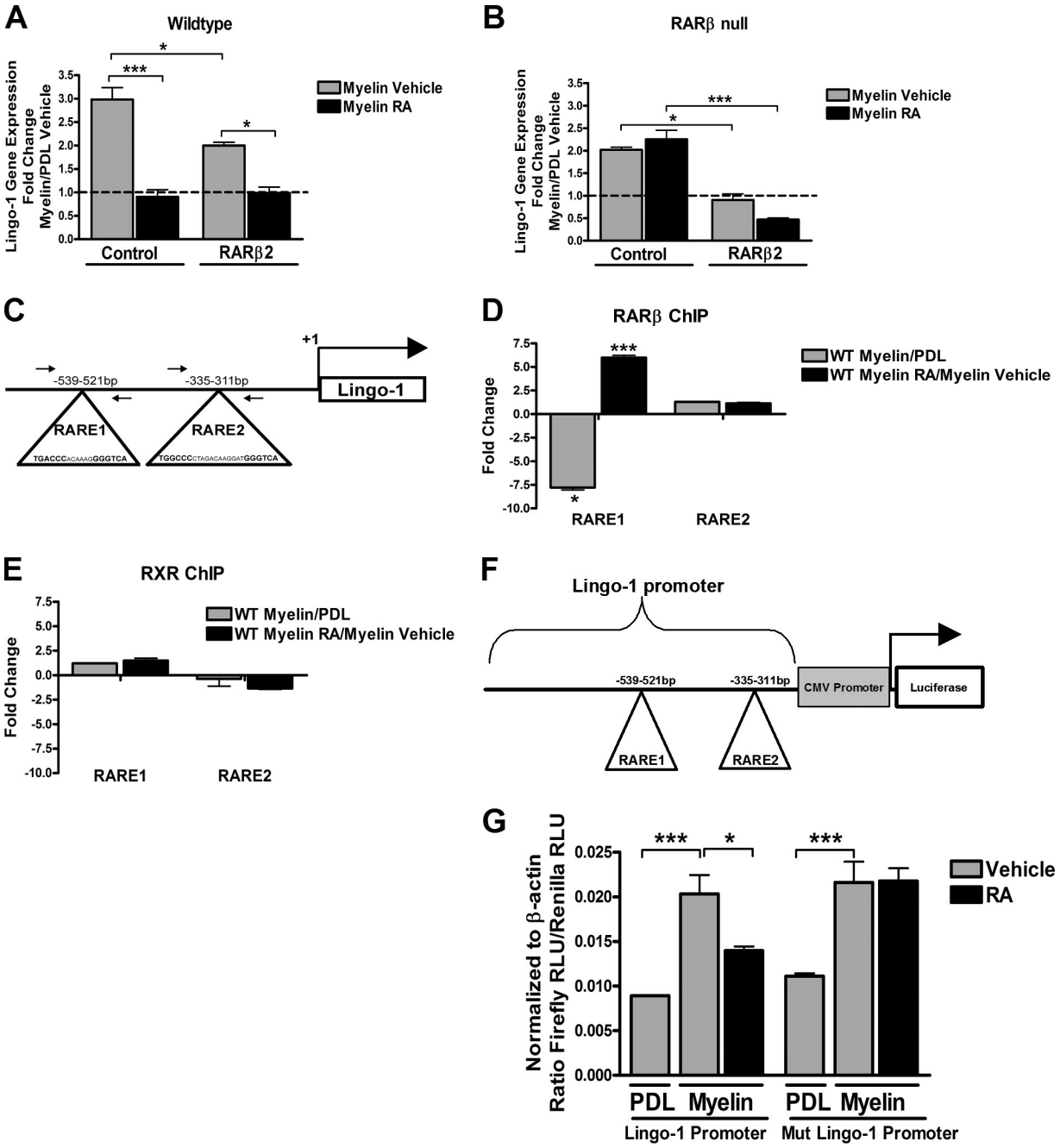

Figure 3. **RAR-β occupies a novel RARE on the Lingo-1 promoter and represses Lingo-1 expression.** (A) Real-time RT-PCR gene expression analysis of Lingo-1 in wild-type CGNs transfected with RAR-β2 plated on myelin versus PDL with vehicle or RA. RA represses Lingo-1 gene expression with a similar pattern to that observed with both RA and RAR-β2, whereas RAR-β2 alone has a more modest repression. (B) Real-time RT-PCR gene expression analysis of Lingo-1 in RAR-$\beta^{-/-}$ CGNs transfected with RAR-β2 plated on myelin versus PDL revealed a rescue of Lingo-1 inhibition and was further inhibited in combination with RA. (A and B) The dashed lines represent the level of no change (onefold). (C) A diagram of two newly discovered RAREs (bold letters) in the Lingo-1 promoter. Small arrows indicate primer sets used for ChIP assays. (D) A ChIP assay shows a significant decrease in the occupancy of the Lingo-1 RARE1 by RAR-β on myelin in comparison with PDL in wild-type (WT) CGNs and a significant increase in occupancy with RA on myelin versus myelin with vehicle. (E) A ChIP assay shows no significant change in the occupancy of either the Lingo-1 RAREs by RXR on myelin in comparison with PDL or with RA treatment on myelin in wild-type CGNs. Unpaired two-tailed *t* test: *, $P < 0.05$; ***, $P < 0.001$. (F) A diagram of the Lingo-1 luciferase construct. CMV, cytomegalovirus. (G) Transfection of SH-SY5Y cells with RAR-β2 in combination with the Lingo-1 promoter or mutant Lingo-1 promoter luciferase expression plasmid with or without RA (24 h) revealed an increase in both luciferase expression plasmids on myelin versus PDL, but only the Lingo-1 promoter luciferase expression plasmid was attenuated by RA treatment ($n = 3$). RLU, relative light unit. One-way ANOVA Bonferroni posttests: *, $P < 0.05$; ***, $P < 0.001$. Data are plotted as the mean ± SEM.

RARE1 of the Lingo-1 promoter, thereby inhibiting its expression in response to myelin. Given this atypical function for RAR-β in transcriptional repression, without its classical binding partner RXR, it will be of great interest to further determine the RAR-β binding partners, possibly histone deacetylases, involved in Lingo-1 repression on myelin.

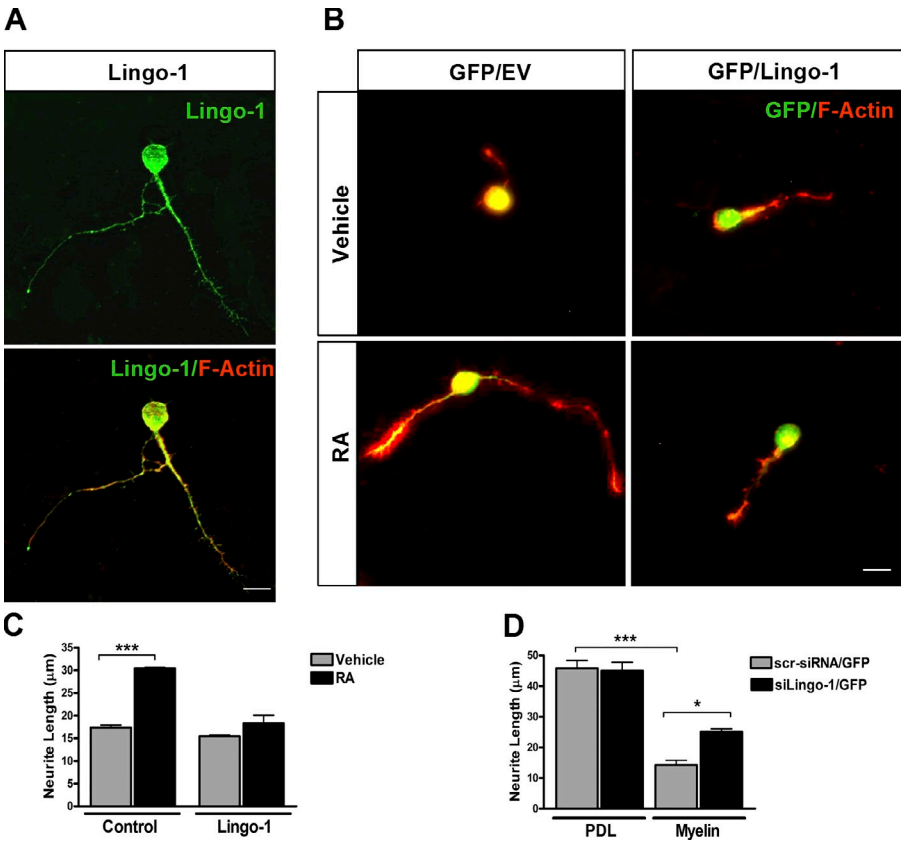

Figure 4. **Lingo-1 overexpression inhibits RA-dependent antagonism of myelin-mediated inhibition of neurite outgrowth, and Lingo-1 silencing induces neurite outgrowth on myelin.** (A) Immunocytochemistry of cultured wild-type CGN on PDL after electroporation with Lingo-1 shows lack of inhibitory effects. Bar, 20 µm. (B) Immunocytochemistry of wild-type CGN on myelin after electroporation (24 h) with GFP–Lingo-1 or GFP–empty vector (EV). Bar, 20 µm. (C) On myelin, control but not Lingo-1 electroporated wild-type CGN with RA treatment (24 h) counteracted myelin-induced inhibition of neurite outgrowth (in triplicate, 60–70 cells/group). One-way ANOVA Bonferroni posttests: ***, $P < 0.001$. (D) Wild-type CGNs were cultured on PDL or myelin after coelectroporation with either scrambled siRNA/GFP or siLingo-1/GFP for 24 h for quantification of neurite length. Myelin inhibition of neurite outgrowth was significantly counteracted in siLingo-1/GFP but not scrambled siRNA (scr-siRNA)/GFP. Neurite length analysis was performed in triplicate (100 cells/group). One-way ANOVA Bonferroni posttests: *, $P < 0.05$; ***, $P < 0.001$. Data are plotted as the mean ± SEM.

RA–RAR-β protects from myelin-dependent inhibition by inhibiting Lingo-1

To ascertain whether the RA–RAR-β pathway counteracts myelin-dependent inhibition of neurite outgrowth selectively through Lingo-1, we overexpressed mouse Lingo-1 in CGNs cultured on myelin to rescue RA-induced Lingo-1 inhibition. These experiments were performed in CGNs treated with RA or vehicle for 24 h; thereafter, neurite length was measured. We observed that the overexpression of Lingo-1 on PDL did not affect neurite outgrowth (Fig. 4 A), as neurite lengths were not significantly different between control and Lingo-1–transfected neurons (not depicted). However, Lingo-1 overexpression on myelin (Fig. 4 B) is sufficient to fully abolish RA-dependent inhibition of neurite outgrowth in wild type but did not substantially affect neurite outgrowth in the absence of RA (Fig. 4, B and C; and Fig. S2). Furthermore, Lingo-1 gene silencing experiments, which repressed Lingo-1 expression at both the mRNA and protein level (Fig. S3, A and B), enhanced neurite outgrowth similar to that of RA treatment alone (Fig. 4 D). These data confirm that the protective role of RA–RAR-β in neurite outgrowth on an inhibitory myelin substrate involves Lingo-1 inhibition.

RA-RAR-β inhibits Lingo-1 expression in vivo after a dorsal overhemisection lesion

It has been established that the inhibition of Lingo-1 or RhoA activation, as well as the overexpression of RAR-β2 or the administration of an RAR-β agonist, promotes axonal sprouting and functional recovery after spinal cord injury (SCI; Dubreuil et al., 2003; Fournier et al., 2003; Mi et al., 2004). Interestingly, the administration of RA not only activates the transcription factor RAR-β but also increases its gene expression (Fig. S1 B; Sucov et al., 1990). What remains to be determined is whether RA will repress Lingo-1 expression after SCI, as this would have relevant implications for the described proregenerative role of RA–RAR-β pathways. Furthermore, it would provide physiological validation of the novel molecular link we have described here in vitro. Indeed, observations from an in vivo study in rats 14 d after SCI (Mi et al., 2004) and our own in vitro work that myelin induces Lingo-1 expression suggest that Lingo-1 expression would be increased in vivo in mice after SCI. However, we did not observe such an increase (Fig. 5, A and B), likely because of the already high basal level of Lingo-1 in the spinal cord. This result is also consistent with another study that shows no change in Lingo-1 expression in mice hours to days after SCI in supraspinal neurons (Barrette et al., 2007). More importantly, we show that Lingo-1 expression is repressed by RA treatment (5 mg/kg daily via intraperitoneal [IP] injection) versus vehicle (DMSO) after a dorsal overhemisection (Fig. 5, A and B). Underlining the importance of Lingo-1 repression is the fact that the presence of all three members of the NgR complex is necessary for RhoA activation (Mi et al., 2004; Park et al., 2005; Shao et al., 2005; Ji et al., 2006). Moreover, Lingo-1 repression is not observed in RAR-$\beta^{-/-}$ mice. These in vivo data provide physiological relevance to the novel molecular mechanism we have elucidated in vitro.

Our findings identify for the first time a direct link between the neuronal proneurite outgrowth RA–RAR-β pathway

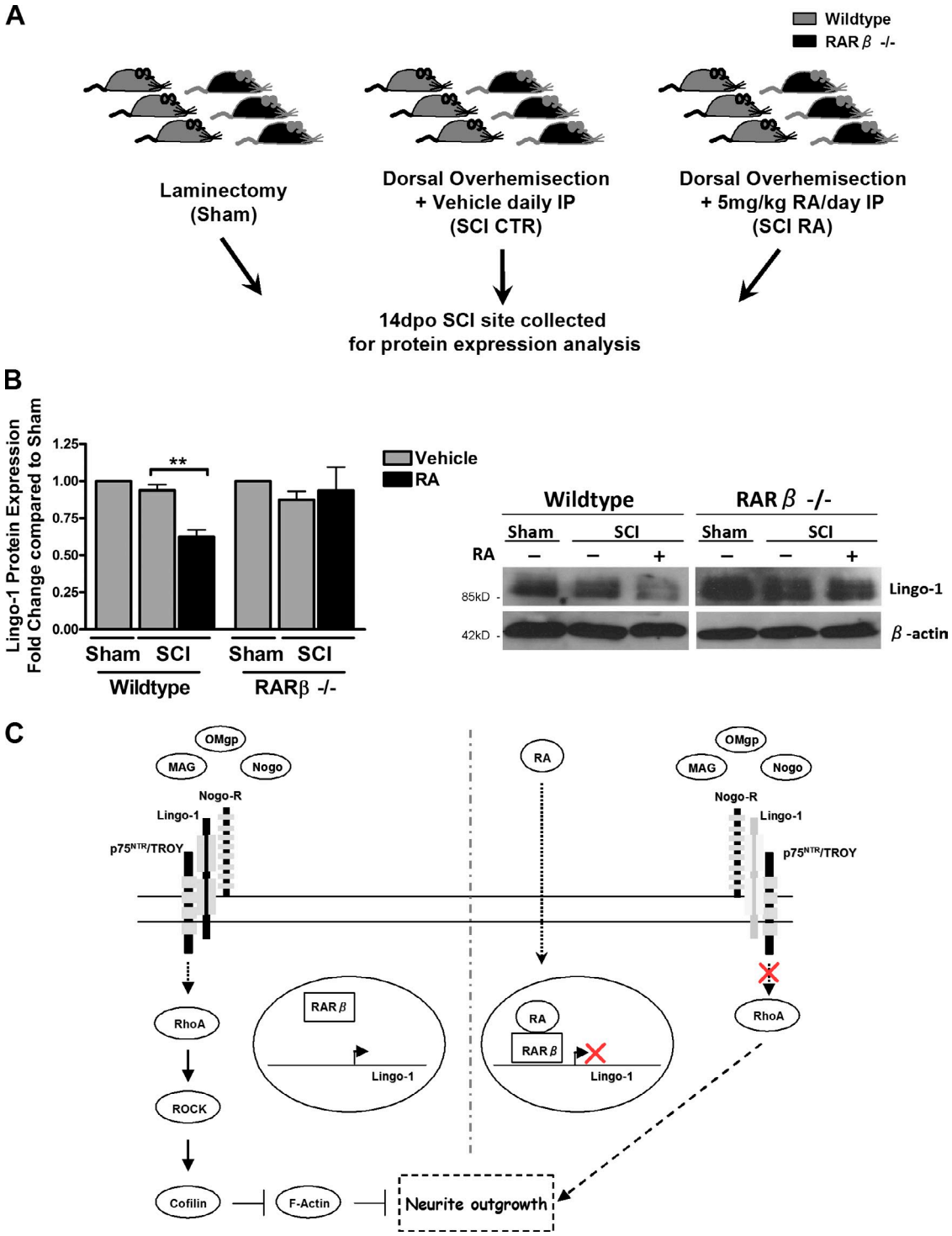

Figure 5. **In vivo RA–RAR-β inhibits Lingo-1 expression after SCI.** (A) A laminectomy (Sham) or T8 dorsal overhemisection lesion was performed on either wild-type or RAR-β$^{-/-}$ mice (n = 3 per group) with vehicle (DMSO) or 5 mg/kg RA daily IP injections after injury (SCI control or SCI RA). dpo, days post operation. (B) Representative immunoblot analysis of the SCI site showed that RA significantly repressed Lingo-1 expression in wild-type but not RAR-β$^{-/-}$ mice (n = 3 per group). One-way ANOVA Bonferroni posttests: **, $P < 0.01$. All data are plotted as the mean ± SEM. (C) A comprehensive diagram of the results presented in this paper shows the role of RA–RAR-β in transcriptionally repressing the NgR signaling pathway, thus leading to neurite outgrowth. RAR-β occupies a novel RARE on the Lingo-1 promoter, thereby repressing Lingo-1 expression. This leads to a decrease in myelin-dependent RhoA activation and neurite outgrowth. OMgp, oligodendrocyte myelin glycoprotein; ROCK, Rho kinase.

and extrinsic inhibitory NgR complex–dependent signaling. We show that RA-bound RAR-β occupies a novel RARE on the Lingo-1 promoter, transcriptionally repressing Lingo-1 gene activation and thus RhoA activation, culminating in neurite outgrowth (Fig. 5 C). This is the first report of transcriptional regulation of an NgR complex member, suggesting that transcriptional control plays a critical functional role for at least one NgR complex member, Lingo-1. Furthermore, we demonstrate

that Lingo-1 expression is required for RA–RAR-β to counteract myelin-dependent inhibition of neurite outgrowth. Finally, we provide physiological confirmation that RA represses Lingo-1 expression in vivo after SCI in an RAR-β–dependent manner. These findings are consistent with, yet further develop, earlier studies that showed a role for RAR-β2 in promoting axonal regeneration after SCI (Corcoran et al., 2002; Wong et al., 2006; Yip et al., 2006). Given that RA and the regenerative molecule cyclic AMP (Qiu et al., 2002) induce expression of RAR-β (Sucov et al., 1990; Kruyt et al., 1992), it will be of interest to determine their combined regenerative effect. Understanding the precise molecular mechanism involved in induction of neuronal regeneration by RA–RAR-β signaling may allow for more comprehensive combinatorial therapies with clinically available RA, for example with the CSPG inhibitor chondroitinase ABC (chondroitin A, B, and C lyase), for the treatment of SCI.

Materials and methods

Cell culture

CGNs were prepared from the cerebella of 8-d-old wild-type or RAR-$\beta^{-/-}$ (NE75 RAR-$\beta^{L-/L-}$; Chapellier et al., 2002) mice after standard procedures. In brief, the cerebella were collected and incubated for 15 min at 37°C in an ionic medium with 0.025% trypsin and 0.05% DNase I (Sigma-Aldrich). 0.04% trypsin inhibitor (Sigma-Aldrich) was added to the tissue and collected by centrifugation. The subsequent pellet was triturated, centrifuged, resuspended in basal Eagle's medium (Invitrogen), and supplemented with 10% bovine calf serum (Invitrogen), 25 mM KCl, 4 mM glutamine, and 100 ng/ml gentamycin. These disassociated CGNs were plated on either PDL or myelin with 1 µM RA (Sigma-Aldrich) or vehicle (DMSO) for 24 h in a humidified atmosphere of 5% CO_2 in air at 37°C. The SH-SY5Y neuroblastoma cell line was grown in DME supplemented with 10% FBS (Invitrogen), 100 U/ml penicillin, and 100 mg/ml streptomycin (Invitrogen) in a humidified atmosphere of 5% CO_2 in air at 37°C.

Neurite length analysis

Immunofluorescence (DAPI, FITC, and Texas red) was detected using a microscope (Axiovert 200M; Carl Zeiss), and pictures were taken at 10× (0.30 NA; Carl Zeiss) or 20× (LD Achroplan, 0.40 NA; Carl Zeiss) magnification using a charge-coupled device camera (Axiocam MRm; Carl Zeiss) at RT (~22°C) and were acquired by AxioVision software (Carl Zeiss). Neurite analysis and measurements in cultured CGNs were performed using Neurolucida software (MBF Bioscience) in triplicate with 100 cells per triplicate. Neurite length was calculated as the mean neurite length per cell by measuring total neurite length and normalizing it to the number of cells included in the analysis (Tuj1-positive cells at 24 h).

RhoA activation assay

CGNs were plated on PDL and stimulated with 1 µM RA for 24 h. RhoA activity was determined from protein isolated from CGNs using the colorimeteric-based RhoA activation assay biochemistry kit (G-LISA; Cytoskeleton) according to the manufacturer's instructions. In brief, protein was isolated after 1 µg/ml MAG stress for 15 min using the provided cell lysis buffer, and cells were processed rapidly on ice and snap frozen until the time of assay. Lysates were clarified by centrifugation at 10,000 rpm at 4°C for 2 min. Protein concentration was determined according to the manufacturer's protocol, and cell extracts were equalized to contain protein concentrations of 0.41 µg/µl for the assay. RhoA activation was detected with a spectrophotometer (Multiskan Ex; Thermo Fisher Scientific).

Overexpression and silencing experiments

Human RAR-β2 (a gift from X.-C. Xu, University of Texas MD Anderson Cancer Center, Houston, TX) and mouse Lingo-1 (Origene) expression constructs were transfected into CGNs via an Amaxa electroporation kit (Lonza) according to the manufacturer's protocol. 3 µg plasmid with 0.75 µg Amaxa EGFP was electroporated (G-013 program) into five to six million CGNs, which were then plated on either PDL or myelin with or without 1 µM RA stimulation for 24 h. The Amaxa EGFP plasmid was used as an electroporation control. For Lingo-1 gene silencing, a combination of two predesigned siRNAs (20 nM) were used (Silencer select IDs 108134 and 108133; Invitrogen). Scrambled siRNAs were used as a control. The efficiency of gene silencing was assessed by real-time RT-PCR and Western analysis after electroporation.

In silico transcription factor binding site analysis

A region of ~2,000 bp of the 5′ untranslated region of the *Lingo-1*, *NogoR1*, *p75^{NTR}*, and *TROY* genes was analyzed using TESS, a search engine which can identify binding sites using site or consensus strings and positional weight matrices from the TRANSFAC database, JASPAR database, Information Matrix Database, and Computational Biology and Informatics Laboratory–GibbsMat database.

ChIP assay

ChIP assays were performed according to the manufacturer's recommendation (17–295; Millipore). In brief, 24 × 10^7 CGNs were grown in the absence or presence of 1 µM RA for 24 h either on PDL or myelin and were subsequently fixed with 1% formaldehyde for 10 min at 37°C. After cell lysis (0.5% SDS, 100 mM NaCl, 50 mM Tris-HCl, pH 8.0, and 5 mM EDTA), extracts were sonicated to shear DNA to lengths of ~200–600 bp. Chromatin solutions were incubated overnight with agitation with 8–10 µg of rabbit polyclonal RAR-β (C-19) X sc-552 (Santa Cruz Biotechnology, Inc.) or rabbit polyclonal RXR (ΔN 197) X sc-774 (Santa Cruz Biotechnology, Inc.). The following day, protein A/G–agarose beads, blocked with salmon sperm DNA, were added to each reaction to precipitate antibody complexes. The precipitated complexes were washed and then incubated for 4 h at 65°C in parallel with input samples to reverse the cross-link. DNA was isolated by phenol/chloroform extraction followed by ethanol precipitation in the presence of sodium acetate. Input, IP, and no-antibody fractions were then analyzed by quantitative PCR (ABI 7000; Applied Biosystems) with appropriate primer pairs for RAREs. The primers used were as follows: Lingo-1 RARE1 forward 5′-CAAGCGGCTCTTGACCTTAG-3′ and reverse 5′-CAAACAGACCCTTCCAGAGG-3′ (201 bp) and Lingo-1 RARE2 forward 5′-GCCAGAGTCCTGAAGAGGTG-3′ and reverse 5′-GCACCCTCCTGTCTGAACAT-3′ (163 bp). For real-time quantitation of PCR products and fold change measurements after ChIP, each experimental sample was normalized to input and no-antibody fractions and was presented as the fold change between individual experimental conditions throughout our results. Three independent experiments in triplicate were evaluated for each condition, and the ΔΔCt method was used for exact fold change assessment as we have previously reported (Tedeschi et al., 2009b).

Luciferase assay

An ~1,000-bp region of the *Lingo-1* proximal promoter containing the RARE1 and RARE2 or a RARE1 mutated sequence was cloned by PCR from genomic DNA of mouse CGNs and ligated into the HindIII and XhoI restriction sites of a luciferase reporter (plasmid 17870; Addgene) for transfection and luciferase experiments. The primers used to clone a 1,000-bp region of the *Lingo-1* proximal promoter containing the RARE1 and RARE2 were forward 5′-CCCAAGCTTTGGCTGGCAGCCCCAGCCTC-3′ and reverse 5′-CCGCTCGAGTGCCTTAGGATCCCTAGAAA-3′. An expression plasmid with a mutated RARE1 sequence was also created by site-directed mutagenesis of this newly cloned luciferase construct (Agilent Technologies). The two overlapping primers carrying seven mutations that were designed using the Stratagene primer design program were sense 5′-CCCAAGTTTGGCTGGCAGCCCCAGCCTCTGAGGTCATCTATGCCAGCCCTGGCGGAAAGGGAGTGAGTCAGGTGTGGAT-3′ and antisense 5′-CCGCTCGAGTGCCTTAGGATCCCTAGAAAAGAGGAGAAACAGGGGAGATCTGTAGGGGTCCATGAGGGACAGAGGGGCTG-3′. Constructs were sequenced to verify the cloned sequences. The mutant sequence within the RARE region that was generated was 5′-AGTTCACAAAGGCTG-3′, versus the wild-type RARE corresponding domain 5′-GACCCACAAAGGGGT-3′. These constructs were then used for transfection experiments. In brief, SH-SY5Y cells were seeded at 350,000 cells per well in a 24-well plate with DME plus 10% FBS, 100 U/ml penicillin, and 100 mg/ml streptomycin 3 h before transfection. Lipofectamine reagent/total DNA ratios were according to standard recommendation, with each well receiving 380 ng Lingo-1Prom-Luc reporter, 380 ng human RAR-β2 plasmid, 20 ng pRL-TK-*Renilla*-luciferase (Promega), and 20 ng EGFP plasmid (Lonza) for a total of 800 ng of total DNA. Upon transfection, some wells were stimulated with 1 µM RA (Sigma-Aldrich) for 24 h. After a 24-h incubation, cells were harvested and lysed with 100 µl of passive lysis buffer, and luciferase activities were determined using the Dual-Luciferase kit (Promega).

Immunocytochemistry

Glass coverslips were coated with PDL at 0.1 mg/ml for 1 h at 37°C. For myelin experiments, these glass coverslips were additionally coated with 4 µg/cm^2 myelin extracted from rat spinal cords for 2 h at 37°C (Gaub et al., 2010). Cells were plated on coated coverslips with or without 1 µM RA (Sigma-Aldrich) for 24 h, at which time they were fixed with 4% paraformaldehyde/4% sucrose. For immunocytochemistry, cells were permeabilized with 0.25% Triton X-100 in PBS for 5 min and then blocked with 1% BSA in PBS and 0.001% Tween. Cells were incubated overnight at 4°C with the primary antibody, mouse anti–βIII Tubulin (Promega). The following day, cells were incubated for 30 min at RT with Alexa Fluor 568–phalloidin (Invitrogen) to visualize F-actin. After a brief rinse with PBS, the sections were incubated with FITC–Alexa Fluor 488 goat anti–mouse IgG secondary antibody (Thermo Fisher Scientific). To visualize each individual cell, we stained the nucleus with Hoechst 3325 (Invitrogen), rinsed the cells with PBS, and mounted them on slides with FluorSave (EMD). For Fig. 4 A, immunofluorescence (band pass 515/30 for FITC and band pass 590/60 for Texas red) was detected using a confocal microscope (LSM 510, Axiovert 200M; Carl Zeiss), and pictures were taken at 20× (Plan-NEOFluar, 0.50 NA) magnification at RT (~22°C) and acquired by AIM software (Carl Zeiss).

Immunoblotting

For immunoblotting, cultured CGNs were collected at 24 h after plating and were lysed on ice for 30 min in a solution containing 10 mM Tris-HCl, 1% Nonidet 40, 150 mM NaCl, 0.1% SDS, and 1% deoxycholate, pH 7.4, containing protease inhibitors (Complete Mini; Roche). The samples were then processed for immunoblotting as previously reported (Gaub et al., 2010) according to standard procedures. Rabbit polyclonal Lingo-1 (Millipore), mouse anti–β-actin (Sigma-Aldrich), and mouse anti–glyceraldehyde-3-phosphate dehydrogenase (Millipore) were used as primary antibodies. Quantitation of protein expression was performed by densitometry (Photoshop; Adobe) of the representative bands of the immunoblots and normalized to the respective levels of β-actin.

Quantitative real-time RT-PCR analysis

RNA was extracted from CGNs using TRIZOL reagent (Invitrogen), and cDNA was synthesized from 0.5 µg of total RNA using both oligo(dT) and random hexamers from the SuperScript II Reverse Transcription kit (Invitrogen). Quantities and fold changes were calculated according to the ΔΔCt method in three independent experiments performed in triplicate according to the manufacturer's instructions (ABI 7000) and as previously reported (Tedeschi et al., 2009a,b). For real-time RT-PCR, the primers used were Lingo-1 forward 5′-GCCTCAACCTGACATCCCTA-3′ and reverse 5′-TTGCCAGAGACATTGAGCAC-3′ (250 bp); NogoR1 forward 5′-CTGGAGGGTAGCAACACCAT-3′ and reverse 5′-TGCAGCCACAGGATAGTGAG-3′ (207 bp); TROY forward 5′-ATTCCCTCAATCCCGAAAAC-3′ and reverse 5′-GTCCTTTGAGCATCCTGAGC-3′ (178 bp); p75^{NTR} forward 5′-CCCAGAATAGCAACCAGGAA-3′ and reverse 5′-ATCGGAAGTTAGGGGCAAGT-3′ (217 bp); and RPL13A forward 5′-CCCTCCACCCTATGACAAGA-3′ and reverse 5′-CCTTTTCCTTCCGTTTCTCC-3′ (167 bp). RPL13A was used for normalization.

SCI

This study was performed in accordance with the Animal Care and Use Committee of the University of Tuebingen. Surgeries were performed on adult wild-type and RAR-β$^{-/-}$ (Chapellier et al., 2002) mice. A dorsal column overhemisection lesion of the spinal column was performed at thoracic level T8 using a precision steel blade, severing the dorsal columns and the corticospinal tracts. Starting on the injury day, the animals were treated with 5 mg/kg RA or vehicle (DMSO) via IP injection for a consecutive 14 d. 2 wk after injury, the animals were sacrificed to collect the 1-cm SCI site to be processed for immunoblotting analysis of Lingo-1 expression. Three animals per group per genotype were used: laminectomy (Sham), dorsal column lesion treated with vehicle (SCI control), or RA (SCI RA).

Statistical analysis

Data are plotted as the mean ± SEM. All experiments were performed in triplicate. Asterisks indicate a significant difference analyzed by a one-way analysis of variance (ANOVA) with Bonferroni posttests or an unpaired two-tailed *t* test as indicated (*, $P < 0.05$; **, $P < 0.01$; ***, $P < 0.001$).

Online supplemental material

Fig. S1 shows that RA does not affect CGN survival. It also shows that RA induces RAR-β expression on myelin, an induction not observed in RAR-β$^{-/-}$ CGN. Finally, Fig. S1 shows that RA does not overcome CSPG inhibition in CGN. Fig. S2 further demonstrates that Lingo-1 overexpression counteracts RA-induced neurite outgrowth on myelin. Fig. S3 shows a significant decrease in both Lingo-1 gene and protein expression after 24 h of Lingo-1 silencing in CGNs. Online supplemental material is available at http://www.jcb.org/cgi/content/full/jcb.201102066/DC1.

We are grateful to Dr. Xiao-chun Xu for providing the human RAR-β2 plasmid. We thank Bernd Knöll, Andrea Wizenmann, Ellen Batchelder, and Khizr Rathore for feedback regarding the manuscript. We also acknowledge Anja Wuttke for technical assistance in CGN extraction and myelin preparation and David Schöndorf for acquiring confocal images. Finally, we would like to thank Sergio Schinelli for his precious technical and conceptual contribution.

This work was supported by the Hertie Foundation and the National Institutes of Health grants R21 NS052640 and DFG DI 1497/1-1 (all granted to S. Di Giovanni).

Submitted: 11 February 2011
Accepted: 25 May 2011

References

Agudo, M., P. Yip, M. Davies, E. Bradbury, P. Doherty, S. McMahon, M. Maden, and J.P. Corcoran. 2010. A retinoic acid receptor beta agonist (CD2019) overcomes inhibition of axonal outgrowth via phosphoinositide 3-kinase signalling in the injured adult spinal cord. *Neurobiol. Dis.* 37:147–155. doi:10.1016/j.nbd.2009.09.018

Barrette, B., N. Vallières, M. Dubé, and S. Lacroix. 2007. Expression profile of receptors for myelin-associated inhibitors of axonal regeneration in the intact and injured mouse central nervous system. *Mol. Cell. Neurosci.* 34:519–538. doi:10.1016/j.mcn.2006.12.004

Bregman, B.S., E. Kunkel-Bagden, L. Schnell, H.N. Dai, D. Gao, and M.E. Schwab. 1995. Recovery from spinal cord injury mediated by antibodies to neurite growth inhibitors. *Nature*. 378:498–501. doi:10.1038/378498a0

Caroni, P., T. Savio, and M.E. Schwab. 1988. Central nervous system regeneration: oligodendrocytes and myelin as non-permissive substrates for neurite growth. *Prog. Brain Res.* 78:363–370. doi:10.1016/S0079-6123(08)60305-2

Chambon, P. 1996. A decade of molecular biology of retinoic acid receptors. *FASEB J.* 10:940–954.

Chapellier, B., M. Mark, J.M. Garnier, M. LeMeur, P. Chambon, and N.B. Ghyselinck. 2002. A conditional floxed (loxP-flanked) allele for the retinoic acid receptor alpha (RARalpha) gene. *Genesis*. 32:87–90. doi:10.1002/gene.10071

Chen, M.S., A.B. Huber, M.E. van der Haar, M. Frank, L. Schnell, A.A. Spillmann, F. Christ, and M.E. Schwab. 2000. Nogo-A is a myelin-associated neurite outgrowth inhibitor and an antigen for monoclonal antibody IN-1. *Nature*. 403:434–439. doi:10.1038/35000601

Corcoran, J., P.L. So, R.D. Barber, K.J. Vincent, N.D. Mazarakis, K.A. Mitrophanous, S.M. Kingsman, and M. Maden. 2002. Retinoic acid receptor beta2 and neurite outgrowth in the adult mouse spinal cord in vitro. *J. Cell Sci.* 115:3779–3786. doi:10.1242/jcs.00046

Domeniconi, M., Z. Cao, T. Spencer, R. Sivasankaran, K. Wang, E. Nikulina, N. Kimura, H. Cai, K. Deng, Y. Gao, et al. 2002. Myelin-associated glycoprotein interacts with the Nogo66 receptor to inhibit neurite outgrowth. *Neuron*. 35:283–290. doi:10.1016/S0896-6273(02)00770-5

Dubreuil, C.I., M.J. Winton, and L. McKerracher. 2003. Rho activation patterns after spinal cord injury and the role of activated Rho in apoptosis in the central nervous system. *J. Cell Biol.* 162:233–243. doi:10.1083/jcb.200301080

Encinas, M., M. Iglesias, N. Llecha, and J.X. Comella. 1999. Extracellular-regulated kinases and phosphatidylinositol 3-kinase are involved in brain-derived neurotrophic factor-mediated survival and neuritogenesis of the neuroblastoma cell line SH-SY5Y. *J. Neurochem.* 73:1409–1421. doi:10.1046/j.1471-4159.1999.0731409.x

Fournier, A.E., B.T. Takizawa, and S.M. Strittmatter. 2003. Rho kinase inhibition enhances axonal regeneration in the injured CNS. *J. Neurosci.* 23:1416–1423.

Gaub, P., A. Tedeschi, R. Puttagunta, T. Nguyen, A. Schmandke, and S. Di Giovanni. 2010. HDAC inhibition promotes neuronal outgrowth and counteracts growth cone collapse through CBP/p300 and P/CAF-dependent p53 acetylation. *Cell Death Differ.* 17:1392–1408. doi:10.1038/cdd.2009.216

Glass, C.K., S.M. Lipkin, O.V. Devary, and M.G. Rosenfeld. 1989. Positive and negative regulation of gene transcription by a retinoic acid-thyroid hormone receptor heterodimer. *Cell*. 59:697–708. doi:10.1016/0092-8674(89)90016-0

GrandPré, T., F. Nakamura, T. Vartanian, and S.M. Strittmatter. 2000. Identification of the Nogo inhibitor of axon regeneration as a Reticulon protein. *Nature*. 403:439–444. doi:10.1038/35000226

He, Z., and V. Koprivica. 2004. The Nogo signaling pathway for regeneration block. *Annu. Rev. Neurosci.* 27:341–368. doi:10.1146/annurev.neuro.27.070203.144340

Ji, B., M. Li, W.T. Wu, L.W. Yick, X. Lee, Z. Shao, J. Wang, K.F. So, J.M. McCoy, R.B. Pepinsky, et al. 2006. LINGO-1 antagonist promotes functional recovery and axonal sprouting after spinal cord injury. *Mol. Cell. Neurosci.* 33:311–320. doi:10.1016/j.mcn.2006.08.003

Kruyt, F.A., G. Folkers, C.E. van den Brink, and P.T. van der Saag. 1992. A cyclic AMP response element is involved in retinoic acid-dependent RAR beta 2 promoter activation. *Nucleic Acids Res.* 20:6393–6399. doi:10.1093/nar/20.23.6393

Le Doze, F., D. Debruyne, F. Albessard, L. Barre, and G.L. Defer. 2000. Pharmacokinetics of all-trans retinoic acid, 13-cis retinoic acid, and fenretinide in plasma and brain of Rat. *Drug Metab. Dispos.* 28:205–208.

Li, S., and S.M. Strittmatter. 2003. Delayed systemic Nogo-66 receptor antagonist promotes recovery from spinal cord injury. *J. Neurosci.* 23:4219–4227.

Lipkin, S.M., C.A. Nelson, C.K. Glass, and M.G. Rosenfeld. 1992. A negative retinoic acid response element in the rat oxytocin promoter restricts transcriptional stimulation by heterologous transactivation domains. *Proc. Natl. Acad. Sci. USA*. 89:1209–1213. doi:10.1073/pnas.89.4.1209

Madura, T., T. Yamashita, T. Kubo, M. Fujitani, K. Hosokawa, and M. Tohyama. 2004. Activation of Rho in the injured axons following spinal cord injury. *EMBO Rep.* 5:412–417. doi:10.1038/sj.embor.7400117

Merkler, D., G.A. Metz, O. Raineteau, V. Dietz, M.E. Schwab, and K. Fouad. 2001. Locomotor recovery in spinal cord-injured rats treated with an antibody neutralizing the myelin-associated neurite growth inhibitor Nogo-A. *J. Neurosci.* 21:3665–3673.

Merrill, R.A., J.M. Ahrens, M.E. Kaiser, K.S. Federhart, V.Y. Poon, and M. Clagett-Dame. 2004. All-trans retinoic acid-responsive genes identified in the human SH-SY5Y neuroblastoma cell line and their regulated expression in the nervous system of early embryos. *Biol. Chem.* 385:605–614. doi:10.1515/BC.2004.075

Mi, S., X. Lee, Z. Shao, G. Thill, B. Ji, J. Relton, M. Levesque, N. Allaire, S. Perrin, B. Sands, et al. 2004. LINGO-1 is a component of the Nogo-66 receptor/p75 signaling complex. *Nat. Neurosci.* 7:221–228. doi:10.1038/nn1188

Miano, J.M., and B.C. Berk. 2000. Retinoids: versatile biological response modifiers of vascular smooth muscle phenotype. *Circ. Res.* 87:355–362.

Park, J.B., G. Yiu, S. Kaneko, J. Wang, J. Chang, X.L. He, K.C. Garcia, and Z. He. 2005. A TNF receptor family member, TROY, is a coreceptor with Nogo receptor in mediating the inhibitory activity of myelin inhibitors. *Neuron*. 45:345–351. doi:10.1016/j.neuron.2004.12.040

Qiu, J., D. Cai, H. Dai, M. McAtee, P.N. Hoffman, B.S. Bregman, and M.T. Filbin. 2002. Spinal axon regeneration induced by elevation of cyclic AMP. *Neuron*. 34:895–903. doi:10.1016/S0896-6273(02)00730-4

Schoorlemmer, J., A. van Puijenbroek, M. van Den Eijnden, L. Jonk, C. Pals, and W. Kruijer. 1994. Characterization of a negative retinoic acid response element in the murine Oct4 promoter. *Mol. Cell. Biol.* 14:1122–1136.

Schwab, M.E., and P. Caroni. 1988. Oligodendrocytes and CNS myelin are nonpermissive substrates for neurite growth and fibroblast spreading in vitro. *J. Neurosci.* 8:2381–2393.

Shao, Z., J.L. Browning, X. Lee, M.L. Scott, S. Shulga-Morskaya, N. Allaire, G. Thill, M. Levesque, D. Sah, J.M. McCoy, et al. 2005. TAJ/TROY, an orphan TNF receptor family member, binds Nogo-66 receptor 1 and regulates axonal regeneration. *Neuron*. 45:353–359. doi:10.1016/j.neuron.2004.12.050

Sucov, H.M., K.K. Murakami, and R.M. Evans. 1990. Characterization of an autoregulated response element in the mouse retinoic acid receptor type beta gene. *Proc. Natl. Acad. Sci. USA*. 87:5392–5396. doi:10.1073/pnas.87.14.5392

Tedeschi, A., T. Nguyen, R. Puttagunta, P. Gaub, and S. Di Giovanni. 2009a. A p53-CBP/p300 transcription module is required for GAP-43 expression, axon outgrowth, and regeneration. *Cell Death Differ.* 16:543–554. doi:10.1038/cdd.2008.175

Tedeschi, A., T. Nguyen, S.U. Steele, S. Feil, U. Naumann, R. Feil, and S. Di Giovanni. 2009b. The tumor suppressor p53 transcriptionally regulates cGKI expression during neuronal maturation and is required for cGMP-dependent growth cone collapse. *J. Neurosci.* 29:15155–15160. doi:10.1523/JNEUROSCI.4416-09.2009

Thallmair, M., G.A. Metz, W.J. Z'Graggen, O. Raineteau, G.L. Kartje, and M.E. Schwab. 1998. Neurite growth inhibitors restrict plasticity and functional recovery following corticospinal tract lesions. *Nat. Neurosci.* 1:124–131. doi:10.1038/373

Vernet, N., C. Dennefeld, F. Guillou, P. Chambon, N.B. Ghyselinck, and M. Mark. 2006. Prepubertal testis development relies on retinoic acid but not rexinoid receptors in Sertoli cells. *EMBO J.* 25:5816–5825. doi:10.1038/sj.emboj.7601447

Wong, L.F., P.K. Yip, A. Battaglia, J. Grist, J. Corcoran, M. Maden, M. Azzouz, S.M. Kingsman, A.J. Kingsman, N.D. Mazarakis, and S.B. McMahon. 2006. Retinoic acid receptor beta2 promotes functional regeneration of sensory axons in the spinal cord. *Nat. Neurosci.* 9:243–250. doi:10.1038/nn1622

Wong, S.T., J.R. Henley, K.C. Kanning, K.H. Huang, M. Bothwell, and M.M. Poo. 2002. A p75(NTR) and Nogo receptor complex mediates repulsive signaling by myelin-associated glycoprotein. *Nat. Neurosci.* 5:1302–1308. doi:10.1038/nn975

Yamashita, T., and M. Tohyama. 2003. The p75 receptor acts as a displacement factor that releases Rho from Rho-GDI. *Nat. Neurosci.* 6:461–467.

Yip, P.K., L.F. Wong, D. Pattinson, A. Battaglia, J. Grist, E.J. Bradbury, M. Maden, S.B. McMahon, and N.D. Mazarakis. 2006. Lentiviral vector expressing retinoic acid receptor beta2 promotes recovery of function after corticospinal tract injury in the adult rat spinal cord. *Hum. Mol. Genet.* 15:3107–3118. doi:10.1093/hmg/ddl251